IOPscience iopscience.iop.org

Home Search Collections Journals About Contact us My IOPscience

Photoconduction in a polydiacetylene film

This article has been downloaded from IOPscience. Please scroll down to see the full text article.

1995 J. Phys.: Condens. Matter 7 1315

(http://iopscience.iop.org/0953-8984/7/7/013)

View the table of contents for this issue, or go to the journal homepage for more

Download details:
IP Address: 171.66.16.179
The article was downloaded on 13/05/2010 at 11:56

Please note that terms and conditions apply.

J. Phys.: Condens. Matter 7 (1995) 1315–1325. Printed in the UK

Photoconduction in a polydiacetylene film

T Ravindran†, W H Kim‡, A K Jain†, J Kumar† and S K Tripathy‡

† Center for Advanced Materials, Department of Physics, University of Massachusetts, Lowell, MA 01854, USA

‡ Center for Advanced Materials, Department of Chemistry, University of Massachusetts, Lowell, MA 01854, USA

Received 27 April 1994, in final form 3 November 1994

Abstract. Steady state photoconductivity, optical absorption and dark conductivity measurements in thin films of polydiacetylene ((8-butoxycarbonyl)methylurethanyl)-1-(5-pyrimidyl)octa-1, 3-diyne (PDA-BPOD) are reported. Steady state photoconductivity results are discussed within the framework of the one-dimensional Onsager theory of geminate recombination. The photoconductivity action spectrum shows a peak at 1.9 eV and a direct band to band transition above 2.4 eV. The absorption spectrum at 50 K is red shifted with respect to the 300 K spectrum. Dark conductivity studies show that the dominant conduction at high fields is due to Schottky emission with a barrier of 0.65 eV.

1. Introduction

A large number of polydiacetylenes having different side groups (R_1 and R_2) are obtained by solid state polymerization of the monomers (R1–C≡C–C≡C–R_2) (Bloor and Chance 1985). Among these polydiacetylenes, polydiacetylene toluene sulphonate (PDA-TS) forms the best-quality single crystals. Its electronic and optical properties have been widely studied by a number of research groups (Donovan and Wilson 1981a, b, Siddiqui 1980, Lochner *et al* 1976, Batchelder and Bloor 1982). Although the electronic properties of polydiacetylenes are primarily determined by π electrons of the backbone, Yang *et al* (1992) observed that the side groups can strongly influence the photocurrent behaviour. The side groups play an important role in determining the lattice parameters of the monomer crystals and the ability of the monomer crystals to polymerize. The electronic states of the polymer backbone are considerably affected by the nature of the side groups and the defects along the backbone.

Kim *et al* (1994b) recently synthesized an asymmetrically substituted soluble polydiacetylene, which has an aromatic side group attached to the backbone through π conjugated bonds. The π conjugation of the side groups can further enhance the π electron density and the delocalization of the π electrons (Gill 1976). This recently synthesized polydiacetylene ((8-butoxycarbonyl)methylurethanyl)-1(5-pyrimidyl)octa-1, 3-diyne (PDA-BPOD) shows solvatochromic behaviour (Kim *et al* 1994b) and high photoconductivity. Electrical and optical properties of the solution cast polydiacetylene films are reported.

2. Experimental details

The polymer PDA-BPOD was obtained by polymerization of the diacetylenic monomer ((8-butoxycarbonyl)methylurethanyl-1-(5-pyrimidyl)octa-1, 3-diyne (BPOD) by γ irradiation.

0953-8984/95/071315+11$19.50 © 1995 IOP Publishing Ltd

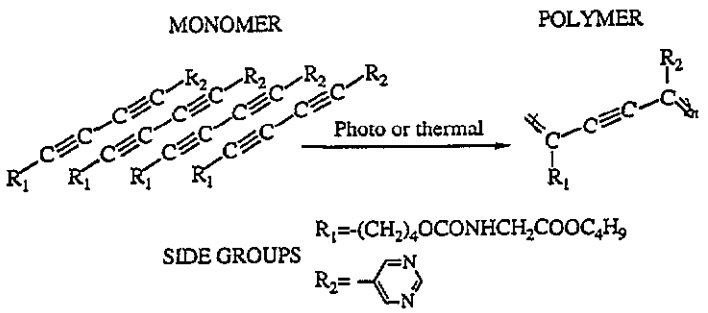

Figure 1. *Solid state polymerization of diacetylenes with a conjugating side group.*

The residual monomer was removed from the polymer using hot methanol. The chemical structure of the polymer is shown in figure 1. The photocurrent dependence on electric field was measured using a surface electrode geometry. All other measurements of photoconductivity and dark conductivity were done in a sandwich geometry.

PDA-BPOD films of thickness ~7 μm were cast from chloroform solution onto a semitransparent gold coated microscopic cover glass. After slow evaporation good-quality films were obtained. The films were kept under vacuum for 4 h to eliminate the residual solvent. A gold electrode of diameter 4 mm was evaporated on top of the cast film by vacuum deposition for measurements in the sandwich geometry. In order to fabricate samples for surface geometry measurements, gold electrodes of separation ~80 μm were made on top of the cast film by vacuum deposition.

The sample was mounted onto a cold finger of a cryostat that can be cooled down to 10 K. CW light from an argon ion laser was chopped at 20 Hz and was used as a light source for 457, 488 and 514 nm. The signal across a 1 MΩ resistor in series with the sample was detected by a lock in detector. The photoconductivity action spectrum was observed in the spectral range of 400–1000 nm. A 50 W tungsten lamp in combination with a monochromator was used. The action spectrum was measured at constant incident light intensity and the data were corrected for transmission through gold.

Low-temperature optical absorption measurements were made using light from a 50 W tungsten lamp and a monochromator. A spin coated film of thickness ~0.1 μm was held by a copper holder with a small hole (~2 mm diameter) and mounted onto the cold finger of a cryostat. The exit slit of the monochromator was adjusted to give a wavelength resolution of 1.5 nm. The transmitted signal was detected by a silicon detector and a lock in amplifier. The signals were recorded by a computer. All the measurements were carried out in a vacuum of 10^{-4} Torr. The room-temperature optical absorption spectra of the spin coated films of thickness ~0.1 μm were obtained from a Perkin Elmer Landa 9 UV/VIS/NIR spectrophotometer. Dark conductivity measurements were made by the two-probe method using an electrometer.

3. Results

PDA-BPOD is a good insulator, having dark conductivity $\sigma \sim 1.1 \times 10^{-12}$ $(\Omega\ \mathrm{cm})^{-1}$. Room-temperature optical absorption spectra and the photoconductivity action spectra are shown in figure 2. The optical absorption spectrum shows a sharp onset at 2 eV and peaks at 2.2 and 2.4 eV. The action spectrum was observed at an electric field (E) of 1.4×10^5 V cm^{-1} and an intensity (I) of 0.0334 mW cm^{-2} in sandwich geometry. Data are corrected for transmission

for gold. The photocurrent (i_p) variation with intensity is linear for all wavelengths. This shows a complete absence of the carrier loss from bimolecular recombination that may occur at shorter penetration depths of the exciting light.

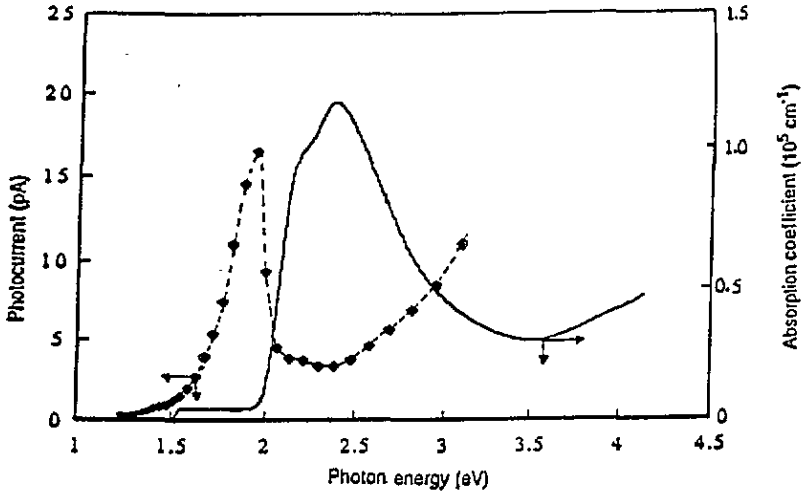

Figure 2. The spectral response of the photocurrent at an electric field of 1.4×10^5 V cm^{-1} and an intensity of 0.0334 mW cm^{-2} and the absorption spectrum at room temperature: ♦, data points; ——, a guide to the eye.

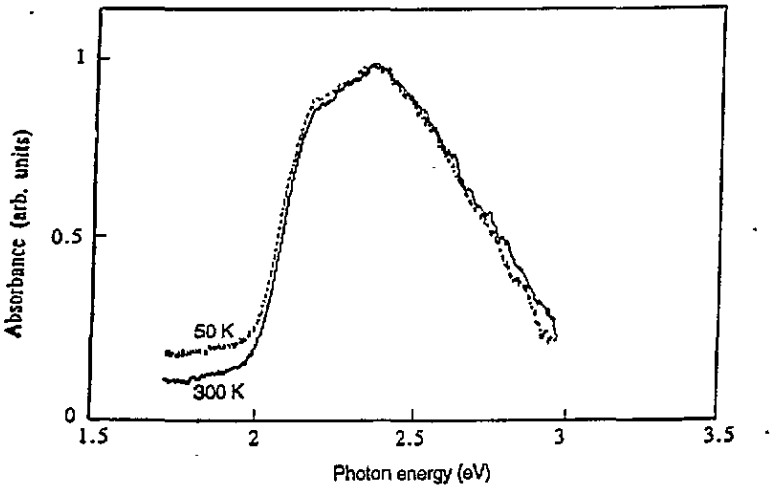

Figure 3. Absorption spectra of a spin coated film at 50 and 300 K.

The onset of the photocurrent action spectrum is at ~15 eV and a peak at 1.9 eV is seen. The photocurrent then decreases and starts increasing again above 2.4 eV. Figure 3 shows the low-temperature absorption spectra. The spectrum at 50 K is red shifted only by about 20 meV with respect to the 300 K spectrum. The oscillator strength of the optical

transition is redistributed to the lower-energy side upon cooling. There is little sharpening in the width of the bands upon cooling. The small change in the absorption spectrum with temperature implies that the broadening is primarily due to the disorder in the spin cast film. Figures 4 and 5 show the intensity dependence of photocurrent at different electric fields and wavelengths respectively. At low intensities (<0.0398 mW cm^{-2}) the photocurrent varies as $I^{1.0}$ followed by a $I^{0.5}$ behaviour at high intensities, indicating a transition from the linear to the bimolecular recombination regime. Figure 6 shows the electric field dependence of the photocurrent at different intensities in the surface electrode geometry. At high fields (>1000 V cm^{-1}) the photocurrent varies linearly with electric field. Deviation from the linear relation is observed at lower fields. The dark current–voltage (i–V) characteristic is shown in figure 7. At high fields (>6000 V cm^{-1}), the log J versus $E^{1/2}$ plot gives a straight line.

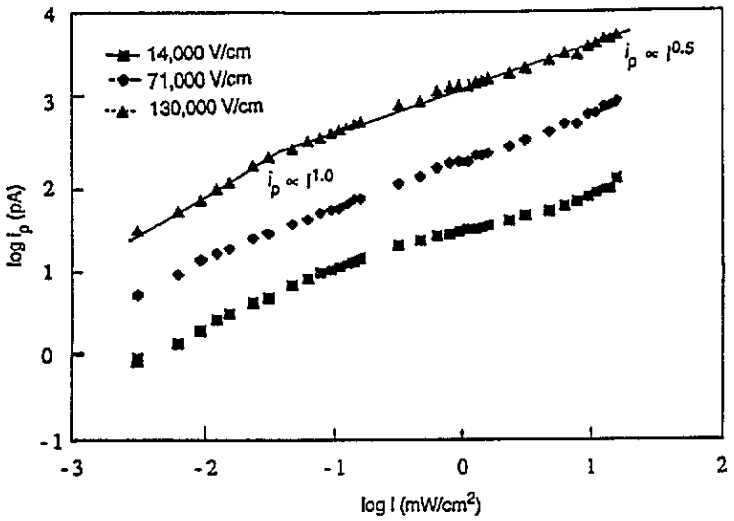

Figure 4. The dependence of photocurrent on intensity at different applied electric fields: wavelength, 488 nm; temperature, 295 K. The solid line represents $i_p \propto I^{1.0}$ at low intensities (<0.039 mW cm^{-2}) and $i_p \propto I^{0.5}$ at high intensities.

The temperature (T) dependence of the steady state photocurrent and dark current (i_d) is shown in figure 8. An Arrhenius plot of log i versus $1000/T$ in figure 9 gives an activated behaviour for both photocurrent and dark current above 200 K. An activation energy of 113 meV is obtained for the photocurrent. Deviation of the photocurrent from the activated behaviour is observed at temperatures below 200 K. The temperature behaviour of the dark current (i_d) gives an activation energy of 311 meV down to 200 K at an electric field of 1.4×10^5 V cm^{-1}. Figure 10 shows a plot of activation energy versus the square root of the applied voltage for the dark current. The activation energy obtained by extrapolating the straight line to zero field is 0.65 eV.

4. Discussion

Optical and electrical properties of conjugated polymers mainly originate from the delocalized π electrons of the backbone of the polymer. Photoexcitation in conjugated

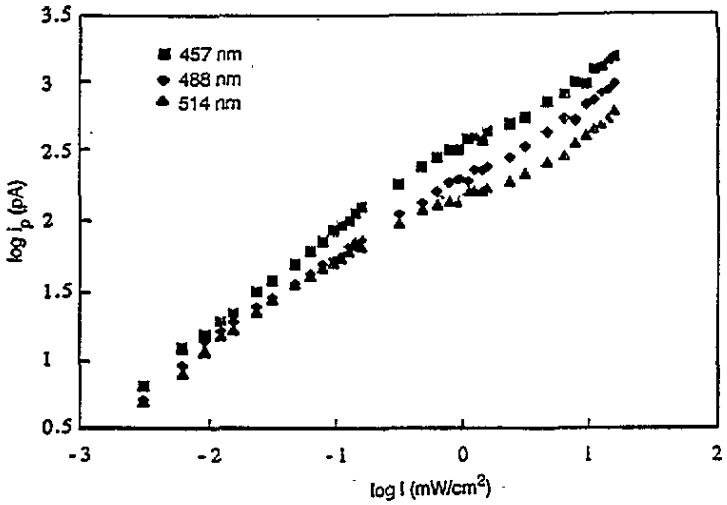

Figure 5. The dependence of photocurrent on intensity at different wavelengths: electric field, 1.3×10^5 V cm^{-1}; temperature, 295 K.

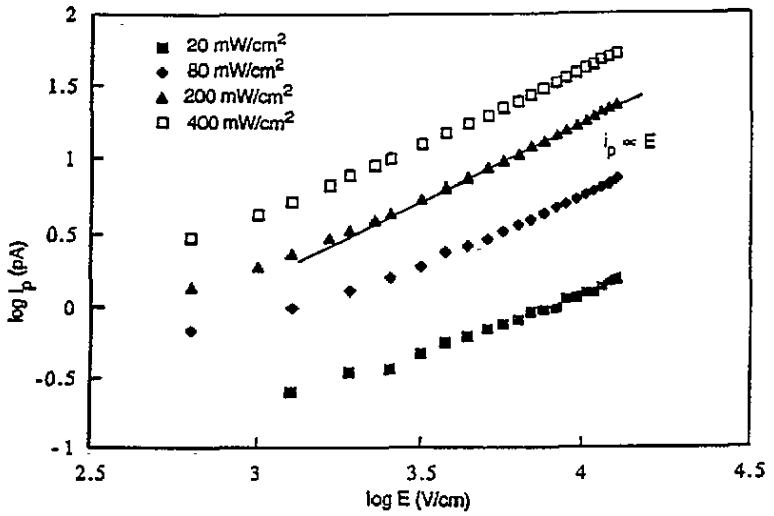

Figure 6. The electric field dependence of the photocurrent at different intensities (surface geometry): wavelength, 488 nm; temperature, 295 K. The solid line corresponds to $i_p \propto E$.

polymers is described in terms of either a band picture of an exciton model depending on the strength of correlation in the photogenerated electron–hole pair. According to the one-dimensional semiconductor band picture of Su and coworkers (1979), photoexcitation above the band gap creates a free electron–hole pair. The strong electron–phonon coupling inherent in one dimension leads to the self-localization of charges in the form of solitons (Su *et al* 1979, Heeger *et al* 1988), polarons and bipolarons (Fesser *et al* 1983) depending on the degeneracy of the ground state system. In the case of degenerate semiconductors such as *trans*-polyacetylenes, solitons are formed, whereas in the case of non-degenerate semiconductors such as polydiacetylenes (Orenstein *et al* 1984, Pratt *et al* 1987, Hattori *et*

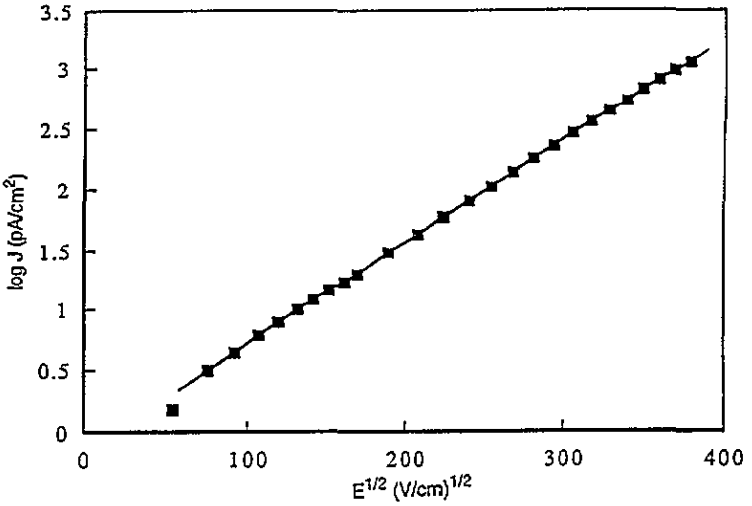

Figure 7. A log J against $E^{1/2}$ plot for the dark current at room temperature. The solid line is a fit to the function $\log J \propto E^{1/2}$.

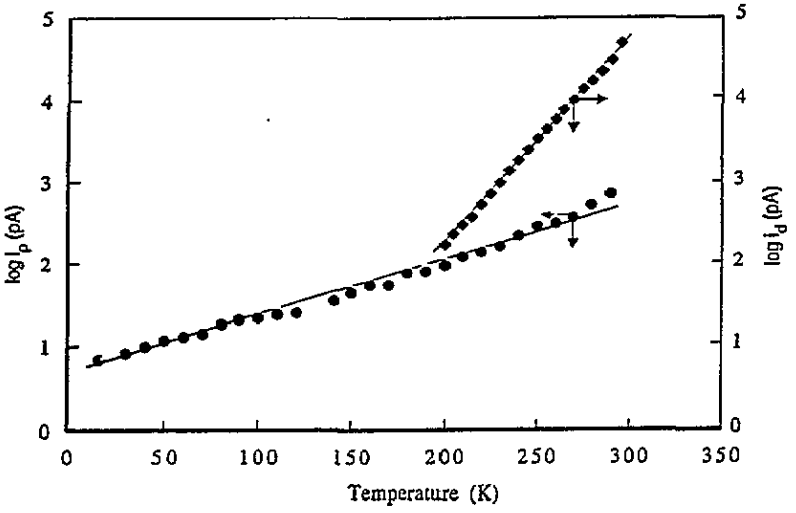

Figure 8. The dependence of photocurrent and dark current on temperature. The solid lines are guides to the eye.

al 1984), poly(p-phenylenevinylene) (Colaneri *et al* 1990), polythiophene (Vardeny *et al* 1986) and polypyrrole (Kanazawa *et al* 1980) polarons and bipolarons are formed. Evidence for this model comes from the midgap absorption observed in photoinduced absorption measurements (Orenstein *et al* 1984, Colaneri *et al* 1990, Vardeny *et al* 1986) and the coincidence of the onset of optical absorption spectra with photoconductivity action spectra (Yu *et al* 1990).

In a certain class of polymers such as poly(phenylenevinylenes) and polythiophenes (Bassler *et al* 1992) an exciton picture is used to describe the optical transitions. Photoconductivity action spectrum (Siddiqui 1980, Lochner *et al* 1978) and electroreflectance

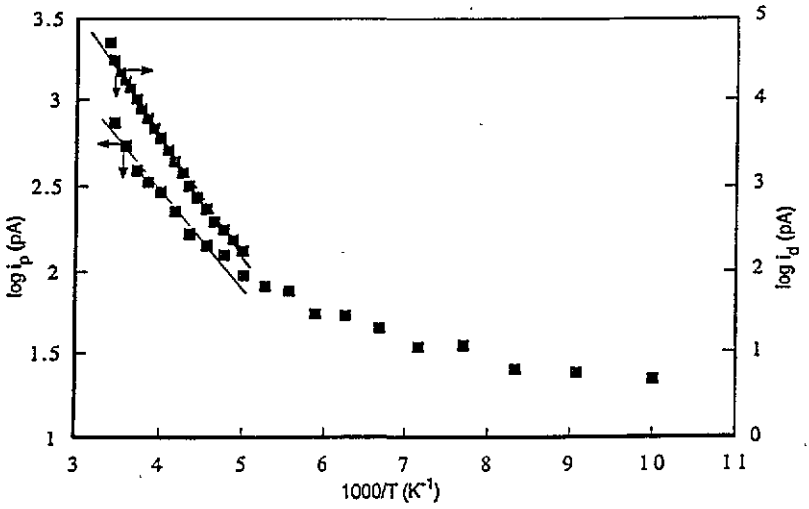

Figure 9. An Arrhenius plot of photocurrent and dark current against temperature. The solid line represents $\log i \propto 1/T$.

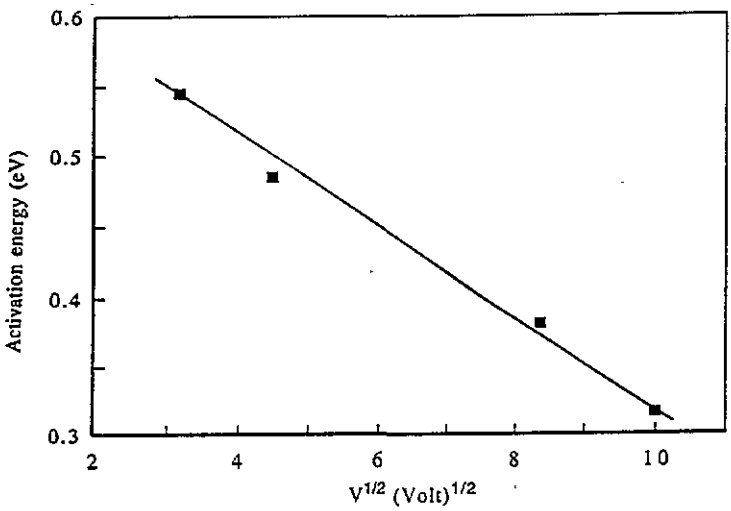

Figure 10. Activation energy versus the square root of the applied voltage for the dark current. The solid line corresponds to a linear fit for activation energy with $V^{1/2}$.

studies (Sebastian and Weiser 1981) of polydiacetylenes confirmed that the dominant optical transition is of excitonic nature with substantial charge transfer. In addition to this, a band to band transition occurs 0.4 eV above the excitonic transition and it is hidden under the dominant excitonic transition (Lochner *et al* 1978).

In a material of low dielectric constant ($\varepsilon = 4$), photocarrier generation of free electron–hole pairs follows the Onsager theory of geminate recombination (Onsager 1938). This theory was originally applied to the dissociation of ion pairs in an electrolytic solution under the combined effect of applied electric field and diffusion. The photocurrent dependence on electric field, wavelength and temperature is successfully explained based on this theory in

molecular crystals such as anthracene (Chance and Braun 1976), amorphous selenium (Pai and Enck 1975) and crystalline polydiacetylenes (Seiferheld *et al* 1983).

Photogenerated hot carriers lose their excess energy and thermalize by phonon emission. In the case of disordered low-dielectric materials ($\varepsilon = 4$) most of the photogenerated carriers form bound electron–hole pairs with an efficiency η. The thermalization distance (a) is related to the activation energy (E_a) for the bound electron–hole pair to escape geminate recombination by

$$a = e^2/(4\pi\varepsilon\varepsilon_0 E_a) \tag{1}$$

where e is the charge of the electron, ε_0 is the permittivity of free space and ε is the relative permittivity. For PDA-BPOD, with $\varepsilon = 4$ and $E_a = 110$ meV, the thermalization distance obtained from equation (1) is 33 Å. The Coulomb capture radius ($r_C = e^2/(4\pi\varepsilon\varepsilon_0 kT)$ is 142 Å at 296 K. Hence hot carriers are thermalized within the Coulomb capture radius. The later process of dissociation of the bound electron–hole pair into free carriers is described by the Onsager model. This model gives the probability of a carrier escaping geminate recombination from the Coulomb field of its partner and the applied electric field. In one dimension this probability is given by (Lochner *et al* 1976, Donovan and Wilson 1981b)

$$\phi = ea^2E/r_C kT \exp(-r_C/a) \qquad a < r_C \qquad E < E_c = kT/(er_C) \tag{2}$$

where k is Boltzmann's constant. The escape probability varies linearly with electric field below a critical field (E_c). Using $r_C = 142$ Å and $T = 296$ K, the critical field obtained for PDA-BPOD is 1.8×10^4 V cm^{-1}. The photocurrent at low light intensities where linear recombination occurs is given by

$$i_p = eN(\eta\phi)(\mu\tau)E/d \tag{3}$$

where N is the number of absorbed photons, μ is the mobility, τ is the linear recombination lifetime of the carriers and d is the electrode separation. A simplified case arises when there is no carrier loss in the bulk of the material, i.e. the carrier lifetime is equal to the carrier transit time ($\tau = d/\mu E$). In this case the photocurrent is a direct measure of the quantum yield ($i_p = eN\eta\phi$). This condition is satisfied in high-quality molecular crystals (Chance and Braun 1976) and PDA-TS single crystals (Donovan and Wilson 1981a). Gailberger and Bassler (1991) applied the same concept to interpret their data on the electric field dependence of the photocurrent in solution cast films of poly(2-phenyl-1,4-phenylenevinylene). The time of flight signals observed in their experiment are evidence in support of the absence of monomolecular recombination of charges.

We assume that most of the photogenerated carriers reach the electrodes in similarly prepared cast films of PDA-BPOD. The molecular weights of these two polymers are equal. An isotropic distribution with chains predominantly distributed in plane is observed in solution cast PDA-BPOD films. Polarized absorption spectra of the spin coated films indicate that the films are isotropic in the in plane direction but anisotropic in the through plane direction (Kim *et al* 1994a). A similar observation was made from the angular and polarization dependence of the second-harmonic signal from the poly(BPOD) thin films. The argument in favour of one-dimensional dissociation of the escape probability originates from the observation that the dominant photogeneration process is intrachain rather than interchain (Friend *et al* 1987). The random orientation of the photogenerated electron–hole pair relative to the applied field may introduce error when treating the one-dimensional problem. Using the data in figure 4 gives a steady state photocurrent density of 5×10^{-9} A cm^{-2} at

$E = 1.3 \times 10^5$ V cm^{-1} and $I = 0.0398$ mW cm^{-2}. Assuming that all the incident photons are absorbed gives a quantum yield $(\eta\phi) = 3 \times 10^{-3}$.

The nature of the optical transition, whether an excitonic or an interband transition, can be obtained by comparing photoconductivity action spectra with optical absorption spectra. The peak at 2.2 eV is ascribed to the lowest singlet exciton of the polymer backbones. The coupling of the electronic transition to the vibrational modes of the backbone leads to the splitting of the electronic level into vibrational side bands. These energies are higher than those of PDA-TS single crystals (Batchelder and Bloor 1982), indicating more conformational disorder in spin coated PDA-BPOD films. Further, the absorption spectrum of spin coated PDA-BPOD films does not show well-resolved vibronic structure as compared to PDA-TS single crystals (Batchelder and Bloor 1982), indicating a distribution of conjugation lengths in PDA-BPOD films. The small red shift of the 50 K absorption spectrum relative to the 300 K spectrum is due to a small increase in conjugation length arising from a decrease of thermal fluctuations at lower temperatures. The reduction in thermal motion of the side groups and the backbone increases the conjugation length of the π electrons of the backbone.

The photocurrent peak at 1.9 eV suggests the excitation of chain defect or impurity states within the band gap. This band is blue shifted compared to the defect band observed in PDA-TS (Siddiqui 1980). A model (DeVore 1956) based on enhanced surface recombination compared to the bulk also predicts a peak in the vicinity of the absorption edge for thick films (thickness larger than the optical absorption depth). The equilibrium charge concentration is greater when the sample is illuminated throughout the bulk of the material. When the sample is illuminated within one absorption depth, the charge carrier concentration is less due to the enhanced surface recombination. This gives rise to a peak near the absorption edge. A combination of these two processes may also be responsible for the peak in the photoconductivity action spectrum. The fact that the photocurrent action spectrum does not follow the optical absorption spectrum implies an absence of exciton dissociation at impurities or the surface to produce free carriers. Further, the short lifetime of the exciton inhibits its thermal ionization. In these disordered polydiacetylene films the band to band excitation energy (2.4 eV) is found to be the same as that of crystalline PDA-TS (Siddiqui 1980). The role of conjugating side groups in modifying the backbone electronic properties is strongly suggested.

The red shift of the photocurrent action spectrum with respect to the absorption spectrum observed in *trans*-$(CH)_x$, which has a degenerate ground state, was interpreted in terms of photogenerated solitons (Etemad *et al* 1981). The photoconductivity action spectrum follows the optical absorption spectrum in poly(3-hexylthiophene). This was interpreted in terms of a direct band to band transition producing free carriers (Yu *et al* 1990). The blue shift of the photoconduction spectra relative to the absorption spectra by 0.5 eV in PDA-TS is due to the Frenkel exciton state below the bottom of the conduction band (Lochner *et al* 1976).

The intensity dependence of the photocurrent shows a transition from a linear to a quadratic bimolecular recombination regime at 0.0398 mV cm^{-2}. At high intensities bimolecular carrier recombination takes place when the distance between an electron and a hole generated by different photons becomes less than the Coulomb capture radius. In the bimolecular regime photocurrent varies as $I^{1/2}$ (Pope and Swenberg 1982).

The one-dimensional Onsager theory of geminate recombination predicts that photocurrent increases linearly with electric field and decreases exponentially with decreasing temperature. Owing to the blocking nature of the electrodes, photogenerated carriers discharge at the electrodes. No carriers are injected from the electrodes to replenish the charge. Based on this condition, photocurrent varies linearly with electric field with the assumption that the majority of the charge carriers reach the electrodes. The deviation from

the linear relation at low fields (<100 V cm^{-1}) may be due to either the finite anisotropy of the jump rates (Ries *et al* 1983) or the contribution of initial interchain electron–hole pairs to the dissociation process (Gailberger and Bassler 1991). A combination of these two processes may also be responsible for the deviation observed at low fields. The activation energy of 113 eV obtained in the temperature dependence of photocurrent corresponds to the energy required for the bound electron–hole pair to escape from its mutual Coulomb field.

The dark current–voltage characteristics of the film show non-Ohmic behaviour at high fields (6000 V cm^{-1}). The low thermal activation energy (311 meV) associated with the temperature dependent dark conductivity eliminates the possibility of a direct band to band transition. In insulating films, non-Ohmic conduction at large fields can arise from either electrode limited Schottky emission or bulk Poole–Frenkel emission. The Richardson–Schottky effect predicts current–voltage characteristics of the form

$$J = AT^2 \exp(-\phi_S/kT) \exp(\beta_S E^{1/2}) \tag{4}$$

with

$$\beta_S = e/kT(e/4\pi\varepsilon\varepsilon_0 d)^{1/2} \tag{5}$$

where A is the Richardson constant and ϕ_S is the Schottky barrier between metal and insulator. Equation (4) predicts a linear relationship between ln J and $E^{1/2}$ with slope β_S. The Poole–Frenkel effect is the field induced thermal ionization from traps in the material. The current–voltage relationship for this mechanism is

$$J = \sigma E \exp(-\phi_{PF}/kT) \exp(\beta_{PF} E^{1/2}) \qquad \beta_{PF} = 2\beta_S \tag{6}$$

where σ is the low-field conductivity and ϕ_{PF} is the energy barrier for the electron to move from the donor level to the conduction band or the valence band to the acceptor level. In the case of the Poole–Frenkel effect the same relation between ln J and $E^{1/2}$ exists but the slope is $2\beta_S$. Using $d = 7$ μm, $\varepsilon = 4$ where n is the refractive index of the material, the β_S value obtained from the graph is 0.33, which is in close agreement with the theoretical value of 0.29 calculated from equation (5). Both the Schottky effect and the Poole–Frenkel model predict a linear relation between the activation energy and the square root of the applied voltage. Lowering of the energy barrier occurs as the voltage increases. Since the experimentally obtained β_S value is in close agreement with the theoretical value, it is reasonable to attribute the zero-field activation energy (0.65 eV) obtained from figure 10 to the Schottky barrier at the metal–polymer interface.

5. Conclusion

The photocurrent dependence on electric field and temperature is discussed based on the one-dimensional Onsager theory of geminate recombination. A peak is observed in the photoconductivity action spectrum at 1.9 eV. A direct band to band transition is observed above 2.4 eV. The optical absorption spectrum at 50 K is red shifted with respect to the 300 K spectrum. Dark conductivity studies show that the conduction at high fields (6000 V cm^{-1}) is due to the Schottky effect.

Acknowledgments

We are grateful to N N Beladakere, S K Sengupta, Bipin Bihari and L Li for helpful discussions. We acknowledge the donors of the Petroleum Research Fund, administered by the ACS, for financial support.

References

Bassler H, Gailberger M, Mahrt R F, Oberski J M and Weiser G 1992 *Synth. Met.* **49&50** 341
Batchelder D N and Bloor D 1982 *J. Phys. C: Solid State Phys.* **15** 3005
Bloor D and Chance R R (ed) 1985 *Polydiacetylenes (NATO ASI Series E 102)* (Dordrecht: Martinus Nijhoff)
Chance R R and Braun C L 1976 *J. Chem. Phys.* **64** 3573
Colaneri N F, Bradley D D C, Friend R H, Burn P L, Holmes A B and Spangler C W 1990 *Phys. Rev.* B **42** 11 670
DeVore H B 1956 *Phys. Rev.* **102** 86
Donovan K J and Wilson E G 1981a *Phil. Mag.* B **44** 9
—— 1981b *Phil. Mag.* B **44** 31
Etemad S, Mitani T, Ozaki M, Chung T C, Heeger A J and MacDiarmid A G 1981 *Solid State Commun.* **40** 75
Fesser K, Bishop A R and Campell D K 1983 *Phys. Rev.* B **27** 4804
Friend R H, Bradley D D C and Townsend P W 1987 *J. Phys. D: Appl. Phys.* **20** 1367
Gailberger M and Bassler H 1991 *Phys. Rev.* B **44** 8643
Gill W D 1976 *Photoconductivity and Related Phenomena* ed J Mott and D M Pai (New York: Elsevier) p 303
Hattori T, Hayes W and Bloor D 1984 *J. Phys. C: Solid State Phys.* **17** L881
Heeger A J, Kivelson S, Schrieffer J R and Su W P 1988 *Rev. Mod. Phys.* **60** 781
Kanazawa K K, Diaz A F, Gill W D, Grant P M, Street G B, Gardina G P and Kwak J F 1980 *Synth. Met.* **1** 329
Kim W H, Bihari B, Moody R, Kodali N B, Kumar J and Tripathy S K 1994a *Macromolecules* at press
Kim W H, Kodali N K, Kumar J and Tripathy S K 1994b *Macromolecules* **27** 1819
Lochner K, Bassler H, Tieke B and Wegner G 1978 *Phys. Status Solidi* **88** 653
Lochner K, Reimer B and Bassler H 1976 *Phys. Status Solidi* b **76** 533
Onsager L 1938 *Phys. Rev.* **54** 554
Orenstein J, Etemad S and Baker G L 1984 *J. Phys. C: Solid State Phys.* **17** L297
Pai D M and Enck R C 1975 *Phys. Rev.* B **11** 5163
Pope M and Swenberg C E 1982 *Electronic Processes in Organic Crystals* (Oxford: Clarendon)
Pratt F L, Wong K S, Hayes W and Bloor D 1987 *J. Phys. C: Solid State Phys.* **20** L41
Ries B, Schonherr, Bassler H and Silver M 1983 *Phil. Mag.* B **48** 87
Sebastian L and Weiser G 1981 *Phys. Rev. Lett.* **46** 1156
Seiferheld U, Ries B and Bassler H 1983 *J. Phys. C: Solid State Phys.* **16** 5189
Siddiqui A S 1980 *J. Phys. C: Solid State Phys.* **13** 2147
Su W P, Schrieffer J R and Heeger A J 1970 *Phys. Rev. Lett.* **42** 1698
Vardeny Z, Ehrenfreud E, Brafman O, Nowak M, Schaffer H, Heeger A J and Wudl F 1986 *Phys. Rev. Lett.* **56** 671
Yang Y, Lee J Y, Kumar J, Jain A K, Tripathy S K, Matsuda H, Okada O and Nakanishi H 1992 *Synth. Met.* **49–50** *439*
Yu G, Phillips S D, Tomozava H and Heeger A J 1990 *Phys. Rev.* B **42** 3004